Preliminary Sizing and Optimization of Semisubmersible Substructures for Future Generation Offshore Wind Turbines

Preliminary Sizing and Optimization of Semisubmersible Substructures for Future Generation Offshore Wind Turbines

Serag-Eldin Abdelmoteleb [a, *], Alejandra S. Escalera Mendoza [b], Carlos R. dos Santos [c], Erin E. Bachynski-Polić [a], D. Todd Griffith [b], Luca Oggiano [c]

[a]*Department of Marine Technology, NTNU, NO-7491 Trondheim, Norway*
[b]*The University of Texas at Dallas, Richardson, Texas, USA*
[c]*Institute for Energy Technology, 2007 Kjeller, Norway*
**Corresponding author email: serageldin.abdelmoteleb@ntnu.no*

Abstract. Several key development areas have been identified as having high potential for reducing the levelized cost of energy of offshore wind. Two of the most anticipated developments are future generation large wind turbines and the use of floating foundations. There is thus a need for developing large floating substructures that are capable of hosting future generation wind turbines. This work presents the preliminary sizing of two semi-submersible platforms for supporting a 25 MW turbine through a design space search using a simplified parametric analysis. Compared to simple theoretical upscaling, the substructures resulting from the proposed simplified parametric analysis have significantly lower steel mass and stiffer tower.

1. Introduction

The trend of rapid growth of wind turbines ratings and sizes to reduce their levelized cost of energy continues unabatedly. Some projections estimate an average wind turbine power rating of 15-20 MW by 2030 [1]. Another anticipated technological development is the use of floating substructures, which may facilitate the transportation and installation of future generation wind turbines. Upscaling reference designs for floating wind turbines (FWTs) provides a good starting point for obtaining preliminary designs for substructures. However, simple theoretical upscaling based on the power ratio may result in unfeasible designs. To avoid this, several studies used simple theoretical upscaling and applied constraints on some geometrical parameters based on static balance and construction requirements [2-4]. The performance of the resulting designs can then be checked using coupled analyses. The problem with this approach is that it does not account for the dynamic behavior of the substructure or the tower in selecting the geometrical parameters of the substructure. This may result in designs with natural frequencies that are close to excitation frequencies, especially for the tower bending modes. Moreover, the upscaled designs may be overly conservative in terms of static stability. Some adjustments to the substructure's geometry might be necessary to obtain better dynamic behavior as suggested by Leimeister et al [2].

Some studies therefore optimize the substructure's geometry based on dynamic models of FWTs. Leimeister et al [5] used a direct optimization method to upscale a reference spar platform initially designed for a 5 MW turbine to host a 7.5 MW turbine. The FWT was modeled using time-domain coupled analysis. The objective of the optimization was to minimize responses in surge and pitch as well as the tower top acceleration in a critical design load condition that was selected based on coupled simulations of the reference platform. The resulting optimum design is likely to depend on the optimization method, the selected design load case, and objectives. In another study by Ferri et al [6], a reference semi-submersible platform designed for a 5 MW turbine was upscaled to host a 10 MW turbine using a parametric study. The study employed a frequency-domain model based on a boundary element solver for modeling hydrodynamic loads and linearized aerodynamic, viscous and mooring loads.

Design selection was based on minimizing rigid body responses and dimensions of the substructure. Significant reductions in responses were obtained compared to theoretically upscaled designs. However, the computational expense of coupled analyses limits the number of parameters and design variations that can be explored. This highlights the need for simplified models for FWTs that can capture their dynamic characteristics with low computational costs.

In this work, rather than using coupled simulations of specified design load cases, a simplified 2D model based on eigenvalue analysis is used to capture the dynamics of FWTs. The model enables exploration of a large design space in a computationally efficient manner; thus, it is used to upscale two reference semi-submersible platforms for supporting a 25 MW wind turbine through a design space search. The objective is to find feasible substructure designs with minimum steel mass and acceptable static responses that satisfy constraints related to the natural periods of rigid motions as well as tower bending modes, which have not been considered in previous upscaling studies. The simplified model and the parametric study used to upscale the reference designs are described in Sections 2 and 3, respectively. Coupled analyses are performed for candidate designs and their results are presented in Section 4.

2. A simplified model for a floating wind turbine

This section presents a simplified approach to model FWTs. The floating system is idealized as a 2D finite element model considering only the degrees of freedom in the vertical-longitudinal plane (i.e., the surge and heave plane) as illustrated in Figure 1. The following subsections describe the contributions of the different components of the FWT to the global inertia and stiffness matrices.

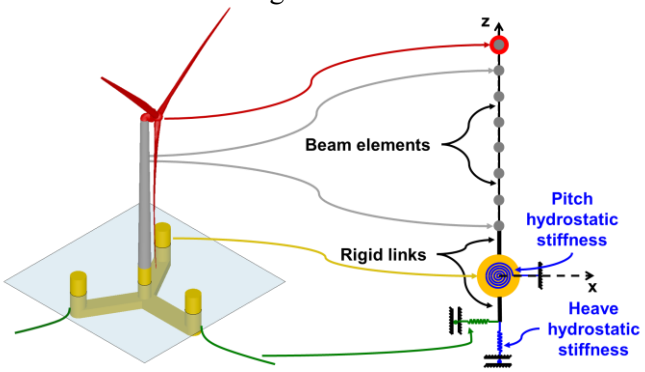

Figure 1 Illustration of the 2D simplified model for a floating wind turbine

2.1. Substructure

The substructure is modelled as a rigid body, represented by a point mass and inertia having three degrees of freedom (surge, heave, and pitch) and located at the mean water line. The mass matrix of the substructure is given by:

$$\mathbf{M_{hull}} = \begin{bmatrix} m_{hull} + A_{11} & 0 & m_{hull}z_{G,hull} + A_{15} \\ 0 & m_{hull} + A_{33} & 0 \\ m_{hull}z_{G,hull} + A_{51} & 0 & I_{yy,hull} + A_{55} \end{bmatrix} \quad (1)$$

where m_{hull} is the mass of the substructure (including steel mass, ballast and tower transition piece), $z_{G,hull}$ is the vertical position of the center of gravity of the hull measured from the mean water line, $I_{yy,hull}$ is the moment of inertia of the substructure about y-axis and the A_{ij} terms represent the added mass of the substructure where the subscripts $i, j \in \{1,3,5\}$ represent the surge, heave and pitch motions, respectively. The added mass terms are calculated by summing up the added mass of the structural components of the hull (pontoons and columns) which are calculated using strip theory by integrating the 2D added mass coefficients over the length of each structural member. The 2D coefficients are obtained from DNV-RP-H103 [7] and adjusted to account for the inclination of the structural members with respect to the global coordinates using a method similar to the one used by Hooft [8].

A vertical translational spring and a torsional spring are used to model the heave and pitch hydrostatic stiffness coefficients, respectively. The hydrostatic stiffness matrix is given by:

$$\mathbf{K_{hs}} = \begin{bmatrix} 0 & 0 & 0 \\ 0 & \rho g A_{wp} & 0 \\ 0 & 0 & \rho g I_{wp} + \rho \nabla g z_B - m_{tot} g z_G \end{bmatrix} \quad (2)$$

where A_{wp} and I_{wp} are the waterplane area and second moment of area around y-axis, respectively, ∇ is the displaced volume, z_B is the vertical position of the center of buoyancy, m_{tot} is the total mass of the FWT and z_G is the vertical position of the center of gravity of the entire floating system.

2.2. Mooring

The mooring system is modelled as a horizontal translational spring located at the fairlead position and connected to the substructure via a rigid link. The stiffness of the spring (k_m) is calculated as the ratio between the maximum thrust of the turbine and a maximum allowable static surge offset of 18 m. This value is selected to give the same static surge offset under rated thrust as the reference FWT platfrom UMaine VolturnUS [9]. The mooring stiffness matrix is given by:

$$\mathbf{K_m} = \begin{bmatrix} k_m & 0 & k_m z_{fair} \\ 0 & 0 & 0 \\ k_m z_{fair} & 0 & k_m z_{fair}^2 \end{bmatrix} \quad (3)$$

where z_{fair} is the vertical position of the fairlead.

2.3. Tower and Rotor Nacelle Assembly (RNA)

The tower is discretized into Euler beam elements with the lowest node located at the freeboard and connected to the substructure via a rigid link. Thus, the horizontal displacement (δ_0) and rotation (θ_0) of the lowest node of the tower are given as functions of the surge (η_1) and pitch (η_5) motions as:

$$\delta_0 = \eta_1 + h_{FB}\eta_5 \quad (4) \qquad \theta_0 = \eta_5 \quad (5)$$

where h_{FB} is the freeboard height. Equations (4) and (5) are used to assemble the mass and stiffness matrices of the substructure and the tower. Finally, the RNA's mass is added to the tower's top node. To assemble the global mass matrix, tower and RNA masses are added to the hull mass in heave.

2.4. Outputs of the simplified model

The main outputs of the simplified model are the natural periods of the floating system obtained from the eigenvalue problem of the global mass and stiffness matrices, and the static pitch under maximum turbine thrust calculated from the following relationship:

$$\begin{bmatrix} k_m & k_m z_{fair} \\ k_m z_{fair} & \rho g I_{wp} + \rho \nabla g z_B - m_{tot} g z_G + k_m z_{fair}^2 \end{bmatrix} \begin{bmatrix} \eta_1 \\ \eta_5 \end{bmatrix} = \begin{bmatrix} F_{thrust} \\ F_{thrust} h_{hub} - m_{RNA} x_{RNA} g - M_{moor} \end{bmatrix} \quad (6)$$

where F_{thrust} is the maximum thrust force of the turbine, h_{hub} is the hub height, m_{RNA} and x_{RNA} are the RNA's mass and upwind distance of its center of mass to the tower top ,respectively, and M_{moor} is the moment resulting from the change in vertical tension in the mooring lines due to an 18 m static surge offset of the FWT from its equilibrium position.

3. Parametric study of two upscaled reference designs

In this section, two reference FWT substructures are upscaled to host a 25 MW wind turbine by conducting a parametric study using the simplified model described in the previous section. The reference platforms chosen for this study are the UMaine VolturnUS platform [9] which is designed to host the IEA 15MW wind turbine [10] on its central column, hereinafter referred to as the central design, and the INO WINDMOOR platform [11] which is designed to host the WINDMOOR 12 MW wind

turbine on one of its peripheral columns, hereinafter referred to as the peripheral design. The 25 MW turbine and tower are theoretically upscaled versions of the IEA 15MW turbine and floating tower with a geometric scaling factor of $\sqrt{25/15}$.

3.1. Parametric study setup

The first step of the parametric study was to parametrize the geometries of the substructures. To be able to describe the mass properties of the substructures in terms of their geometric parameters the following assumptions were made:

- The substructures are made of steel ($\rho_{steel} = 7850\ \mathrm{kg/m^3}$, $E = 200$ GPa) with a constant steel thickness across all structural members. The thickness was back calculated from the UMaine VolturnUS platform as 4.6 cm and theoretically upscaled for the larger 25 MW designs.
- Seawater ballast is placed in the pontoons
- Fixed concrete ballast ($\rho_{conc.} = 2560\ \mathrm{kg/m^3}$) is placed in the side columns for the central tower design and only in two columns in the peripheral tower design to counteract the turbine's weight

The mass properties of the original platforms calculated under the aforementioned assumptions were found to be close to their original values. Figure 2 shows the geometric parameters of the two platform concepts. The parameters are divided into four categories according to how their values were obtained in the parametric study: theoretically upscaled parameters, variable input parameters for the parametric study, derived parameters that are obtained using static balance or geometric constraints, and constant parameters such as fairlead depth (14 m). All the parameters with their description are listed in Table 1.

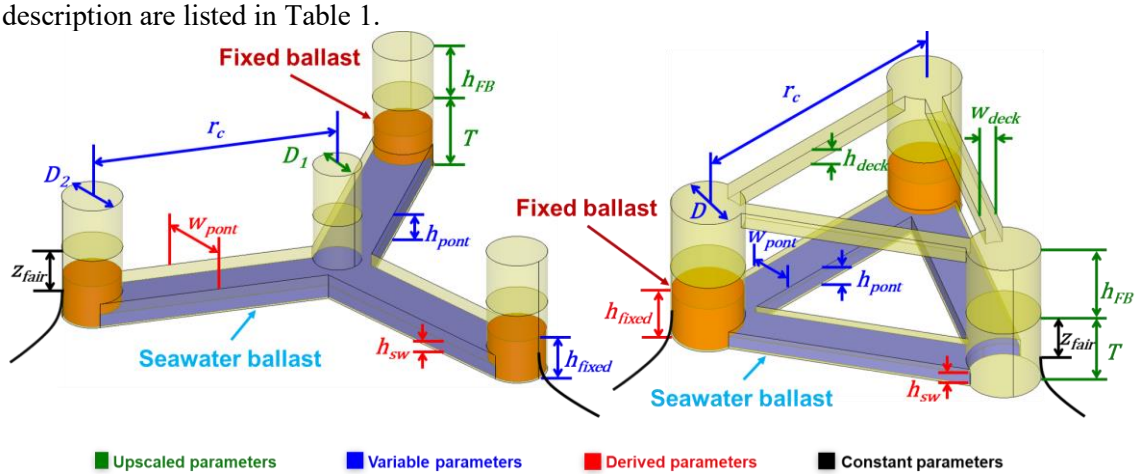

Figure 2 Geometric parameters of the central tower design (left) and peripheral tower design (right)

Table 1 Description of the geometric parameters of the reference platforms

Central design			Peripheral design		
Param.	**Description**	**Category**	**Param.**	**Description**	**Category**
r_c	Center to side column distance	Variable	r_c	Column-column distance	Variable
D_1	Central column diameter	Upscaled	D	Column diameter	Variable
D_2	Side column diameter	Variable	T	Draft	Upscaled
T	Draft	Upscaled	h_{FB}	Freeboard	Upscaled
h_{FB}	Freeboard	Upscaled	w_{pont}	Pontoon width	Variable
w_{pont}	Pontoon width (equals D_2)	Derived	h_{pont}	Pontoon height	Variable
h_{pont}	Pontoon height	Variable	w_{deck}	Deck beam width	Upscaled
h_{fixed}	Fixed ballast height	Variable	h_{deck}	Deck beam height	Upscaled
h_{sw}	Sea water ballast height	Derived	h_{fixed}	Fixed ballast height	Derived
z_{fair}	Fairlead depth	Constant	h_{sw}	Sea water ballast height	Derived
			z_{fair}	Fairlead depth	Constant

The fixed ballast height for the central platform was varied in the parametric study by varying the ratio between the fixed ballast and the total ballast required (bal_{ratio}) to keep the platform at the design draft. To generate the design space the input parameters are varied as a ratio of their theoretically upscaled values, except for the pontoon width for the peripheral design which was varied as a ratio of the column diameter. Scaling factors and the setup of the parametric study are given in Table 2. The upscaled value of the freeboard for the central design is also used for the peripheral design so that the two designs have the same hub height.

Table 2 Parametric study setup

Central design (Scaling factor = $\sqrt{25/15}$)		**Peripheral design (Scaling factor = $\sqrt{25/12}$)**	
Param.	**Range**	**Param.**	**Range**
$r_c/r_{c,upscaled}$	0.5 to 1.5	$r_c/r_{c,upscaled}$	0.5 to 1.5
$D_2/D_{2,upscaled}$	0.5 to 1.5	$D/D_{upscaled}$	0.5 to 1.5
$bal_{ratio}/bal_{ratio,reference}$	0.5 to 1.5	w_{pont}/D	0.5 to 1
$h_{pont}/h_{pont,upscaled}$	0.5 to 1.5	$h_{pont}/h_{pont,upscaled}$	0.5 to 1.5

Unfeasible designs were identified and removed from the design space. Unfeasible designs include those with negative stability (negative pitch restoring moment), insufficient ballast space, or negative ballast.

3.2. Parametric study results

The aim of the parametric study was to find feasible designs that minimize the substructure's steel mass and static pitch under maximum thrust while satisfying the following constraints: (1) a maximum hull dimension of 120 m; (2) minimum rigid body natural periods of 20 s; (3) stiff-stiff floating tower, and (4) less than 30 degrees static pitch.

Since the two objectives of minimizing the substructure's steel mass and static pitch are contradictory, Pareto fronts were used to find designs with minimum steel mass at different maximum allowable static pitch angles. Figure 3 shows the variation of steel mass with maximum allowable static pitch for all feasible design points that satisfy the constraints. The results show that the theoretically upscaled designs have over-conservative low static pitch angles and high steel masses relative to the design space. Moreover, by relaxing the static pitch angle by a few degrees, a significant decrease in the steel mass can be achieved. For example, relaxing the static pitch angle from its value at the theoretically upscaled designs (about 2 degrees) to 6 degrees, which is considered acceptable for a FWT [12], results in a steel mass reduction of about 17% for the central design and about 12% for the peripheral design. The estimated steel mass of the peripheral tower designs is higher than that of the central tower designs due to the existence of deck beams. A detailed structural analysis is thus needed to assess the need for adding deck beams and optimize their dimensions, and to check the integrity of the rest of the hull.

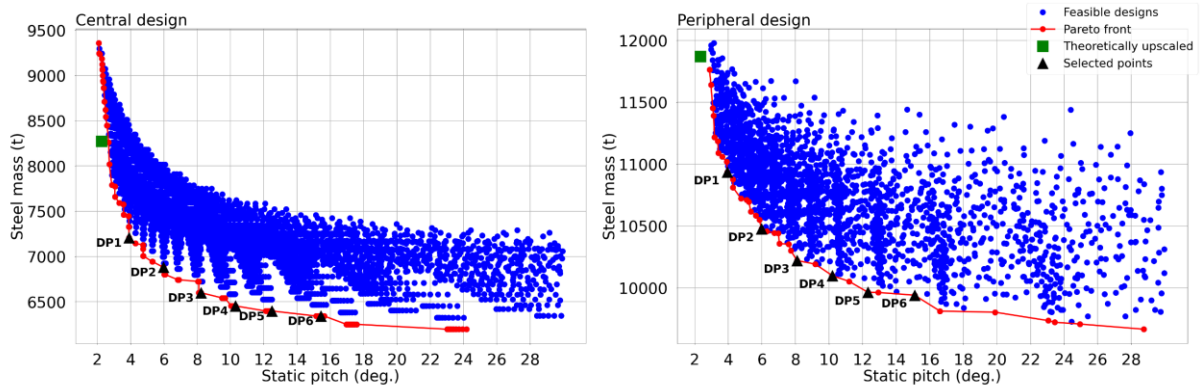

Figure 3 Variation of steel mass with max. static pitch of the central design (left) and peripheral design (right)

Six design points with different static pitch angles along the Pareto fronts were selected for further analyses along with the theoretically upscaled designs. The main horizontal dimensions of the selected design points for both design concepts are given in Figure 4, which also shows contours of the maximum horizontal hull dimension. Generally, the peripheral designs are smaller than the central designs. Additionally, the theoretically upscaled designs are larger than the designs selected along the Pareto front except for one selected design point (DP1) for the peripheral design. Thus, selecting a maximum allowable static pitch of 6 degrees (DP2) will result in significantly smaller designs compared to the theoretically upscaled designs.

Figure 5 shows the variation of the natural periods of the platform's pitch motion and the first tower fore-aft bending mode as a function of the maximum allowable static pitch angle for the selected design points. Naturally, as the allowable static pitch angle increases, the platform becomes less stiff in pitch and its natural period increases. This is generally accompanied by a decrease in the platform's size which affects the boundary conditions at the tower bottom as the mass, pitch moment of inertia, and pitch hydrostatic stiffness decrease. However, the surge stiffness remains constant as the mooring line properties do not change. The net effect of the changes in the boundary conditions at the tower bottom is a stiffer tower as illustrated by the decreasing natural period of the tower's first bending mode.

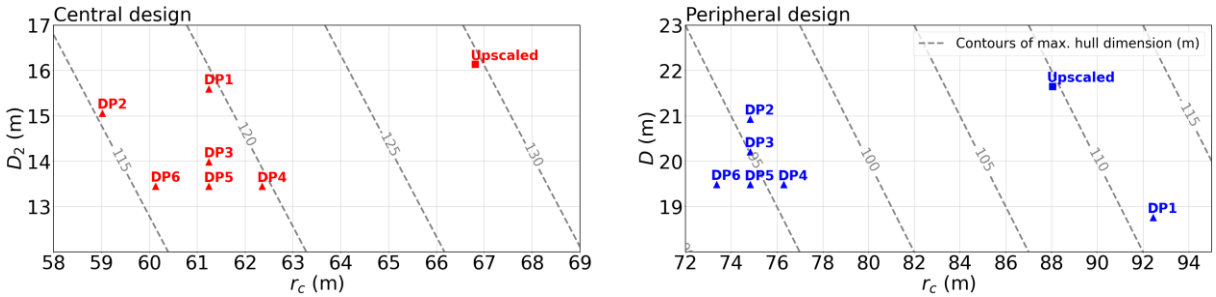

Figure 4 Horizontal dimensions of selected design points of the central design (left) and peripheral design (right)

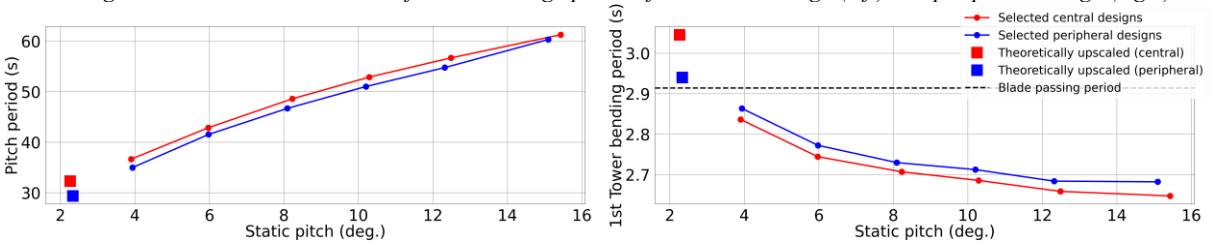

Figure 5 Variation of natural periods of pitch motion and tower fore-aft bending of the selected designs with the maximum allowable static pitch

4. Coupled analysis for selected designs

To verify the results obtained from the simplified model and assess the performance of the generated designs, coupled analyses for the selected design points were conducted using OpenFAST. A 25 MW baseline rotor design was obtained by upscaling the outer geometry of the IEA 15 MW blade [10] based on the power ratio. Then, a detailed structural analysis was performed to define the laminate thicknesses of main load carrying components of the blade to meet strength and frequency requirements of international design standards. The nacelle, tower, and mooring line properties were theoretically upscaled from the UMaine VolturnUS-S reference FWT [9].

4.1. Decay tests

Decay tests for surge, heave, pitch and tower bending were performed for the selected designs using OpenFAST. Tables 3 and 4 summarize the results of the decay tests for the theoretically upscaled designs (DP0) and the six selected designs along the Pareto fronts with varying static pitch angles (DP1-6) for the central and peripheral designs, respectively. The natural frequencies and the static pitch angles under maximum thrust according to the simplified model are also given.

Table 3 Natural frequencies of the selected design points for the central design

DP	Static Pitch (deg)	Surge (Hz)		Heave (Hz)		Pitch (Hz)		Tower FA (Hz)	
		decay	estimated	decay	estimated	decay	estimated	decay	estimated
0	2.3	0.0064	0.0075	0.043	0.0433	0.033	0.031	0.3625	0.3283
1	3.9	0.0079	0.0091	0.0494	0.0491	0.028	0.0273	0.3942	0.3526
2	6	0.0081	0.0093	0.0502	0.0499	0.024	0.0233	0.4106	0.3644
3	8.2	0.0085	0.0096	0.0497	0.0494	0.0214	0.0206	0.4156	0.3694
4	10.3	0.0087	0.0097	0.0494	0.0491	0.0202	0.0189	0.4193	0.3723
5	12.5	0.0088	0.0096	0.0498	0.0495	0.0187	0.0176	0.4242	0.3761
6	15.4	0.0088	0.0094	0.0502	0.0499	0.0174	0.0163	0.4249	0.3777

Table 4 Natural frequencies of the selected design points for the peripheral design

DP	Static Pitch (deg)	Surge (Hz)		Heave (Hz)		Pitch (Hz)		Tower FA (Hz)	
		decay	estimated	decay	estimated	decay	estimated	decay	estimated
0	2.3	0.0067	0.0079	0.051	0.0511	0.0327	0.034	0.3579	0.3401
1	3.9	0.008	0.0094	0.0497	0.0494	0.0265	0.0286	0.3638	0.3492
2	6	0.0076	0.0087	0.0507	0.05	0.0235	0.0241	0.393	0.3607
3	8.1	0.0079	0.0089	0.0506	0.0499	0.0211	0.0214	0.3969	0.3663
4	10.2	0.0081	0.009	0.0501	0.0495	0.0192	0.0196	0.3969	0.3686
5	12.3	0.0081	0.0089	0.0505	0.0498	0.0177	0.0183	0.4023	0.3726
6	15.1	0.0079	0.0087	0.0498	0.0492	0.0164	0.0166	0.4051	0.3728

Good agreement was found for both the heave and pitch natural frequencies with maximum relative percentage errors of 1.4% and 8%, respectively. For the surge motion and the tower fore-aft bending mode, the errors are larger, 18% and 11.2%, respectively. These discrepancies can be attributed to several factors, including the following:

- Differences in the added mass values. The simplified model employs a 2D strip theory approach, while the decay tests rely on hydrodynamic coefficients obtained from the boundary element potential flow solver WAMIT.
- Differences in the mooring models. The simplified model uses a linear mooring stiffness matrix. For the decay tests, 3 catenary mooring lines are modelled using the MoorDyn module in OpenFAST.
- Neglecting the inertia of the RNA in the simplified model

Only design points 0,1, and 2 were tested in wind conditions. The pitch natural frequencies obtained from the decay tests were used to tune the blade pitch controller of the reference controller ROSCO[13]. To avoid the infamous negative pitch damping problem of FWTs, the bandwidth of the blade pitch controller was set to 90% of the pitch natural frequency while also using a proportional constant negative gain on the tower-top pitch angular velocity (the same value was used for all designs). The torque speed controller bandwidth was set to 0.3 rad/s.

4.2. Constant wind tests

The performances of the rotor and the controller were tested in steady wind at different wind speeds by varying the wind speed from the cut-in speed (4 m/s) to the cut-out speed (25 m/s) with 1 m/s step. Each wind speed was kept constant for 600 s and the transition between speeds is linear over 100 s. The tests were performed in calm water, and a quadratic damping matrix was introduced to account for the viscous effects using constant drag coefficients obtained from DNV-RP-H103 [7]. Results of the step wind tests are given in Figures 6 and 7 for the central designs and the peripheral designs, respectively. At below rated speeds, the turbine performs as expected for all designs. The blade pitch controller results in negatively damped surge motion at wind speeds right above the rated speed of 11 m/s. This problem could be avoided by reducing the bandwidth of the blade pitch controller to be less than the surge natural frequency, but this would result in an unrealistically slow controller in real environmental conditions with turbulent wind, where the surge oscillations are less problematic.

The static pitch values at rated conditions are within 0.5 degrees of the estimated values from the simplified model. Apart from the platform motions, all designs have nearly identical performance in constant wind conditions.

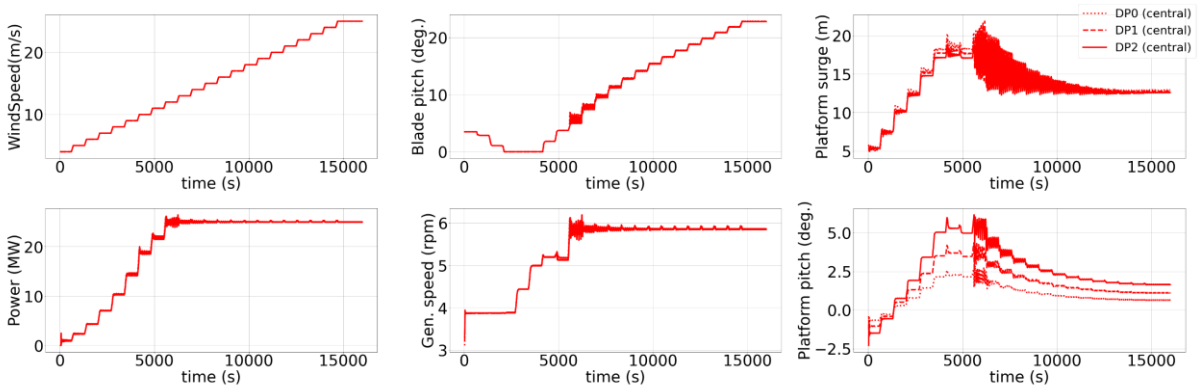

Figure 6 Step wind test results for central tower designs

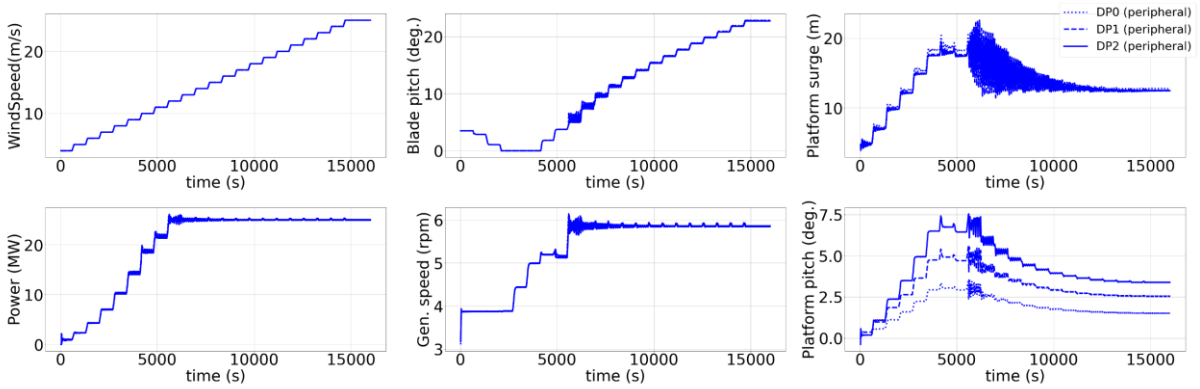

Figure 7 Step wind test results for peripheral tower designs

4.3. Operational conditions tests

Three environmental conditions with turbulent wind and irregular waves were used to test the selected designs during operational conditions. The conditions are summarized in Table 5. One-hour simulations were considered (after removing 1800 s transients).

Table 5 Operational Environmental conditions

Mean wind speed at hub height (*U*)	5 m/s	11 m/s	25 m/s
Significant wave height (H_s)	0.5 m	1.5 m	3.5 m
Peak wave period (T_P)	6.5 s	7.5 s	9 s

The wave conditions were chosen as the most common conditions for the specified mean wind speeds at the Gulf of Maine site [14]. Waves were modeled using a JONSWAP spectrum and wind was modeled using a Kaimal spectrum assuming IEC class C turbulence intensity. Figures 7 to 9 show the response spectra for the surge, heave, and pitch motions along with the fore-aft tower base bending moment.

In the below rated condition, the platform motion responses are mostly influenced by the low frequency wind excitation. Moreover, the frequency of first tower bending mode coincides with the 6P frequency which results in resonant responses in this region. Responses at the rated condition are dominated by surge resonant response due to the negative feedback from the blade pitch controller. Even the heave motion can be excited by the changes in mooring tension due to surge motion or the vertical component of thrust caused by platform pitching. For the above rated condition, large variations in wind speed cause large oscillations in surge due to the slow controller response caused by detuning the

controller based on the pitch natural frequency. This is evident by the fact that the surge response is lowest for designs with highest pitch frequencies (DP0) and highest for designs with lowest pitch frequencies (DP2). The energy content of the tower base bending moment spectra near wave excitation increases as the significant wave height and peak wave period increase. Moreover, the negative feedback and slow controllers result in large variations in rotor speed in the rated and above rated conditions. As a result, the 3P range becomes larger and the energy content of the tower base bending moment spectra increases in this region. This effect is exacerbated for the above rated condition as the 3P range becomes closer to the range of natural frequencies of the first tower bending mode. As the maximum allowable static pitch increases (from DP0 to DP2), the energy content of the tower base bending moment decreases in the 3P range as the natural frequency of the first tower bending mode increases (moves farther away from the 3P range).

The mean values and standard deviations of electrical power output for all the tested designs and environmental conditions are given in Figure 11. Power variation is similar for both the central and peripheral designs. As expected, the rated condition has the highest variability in power due to the negative surge feedback, and as the pitch frequency decreases (from DP0 to DP2) the blade pitch controller becomes slower and hence the power varies more in the above rated condition.

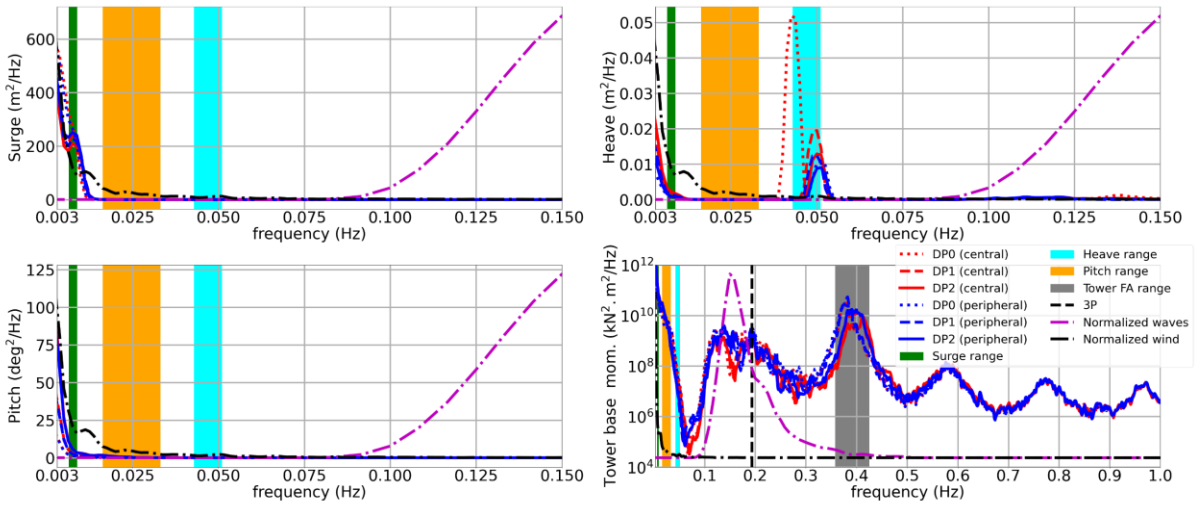

Figure 8 Below-rated condition response spectra (U = 5 m/s, H_s = 0.5 m, T_p =6.5 s)

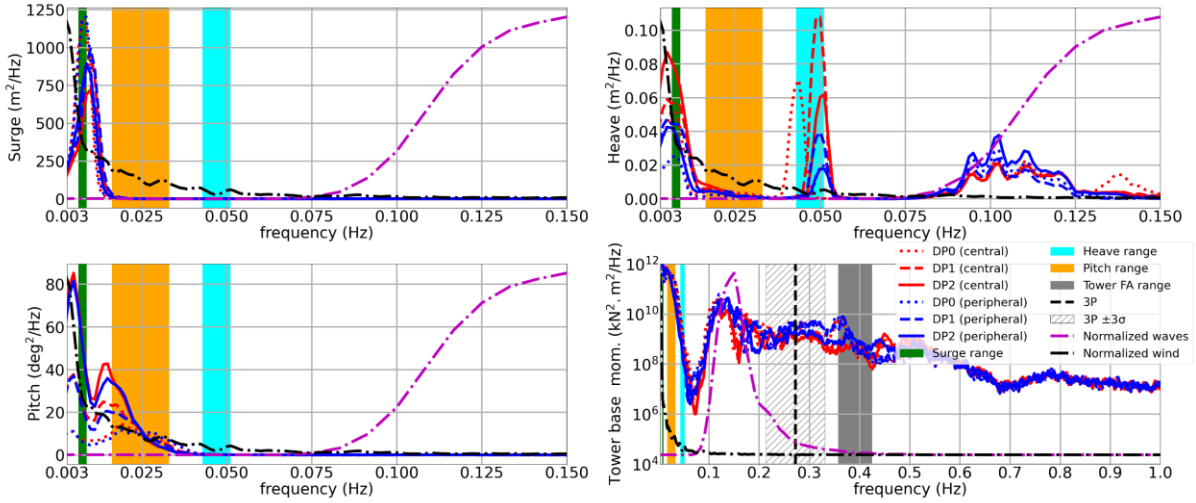

Figure 9 Near-rated condition response spectra (U = 11 m/s, H_s = 1.5 m, T_p =7.5 s)

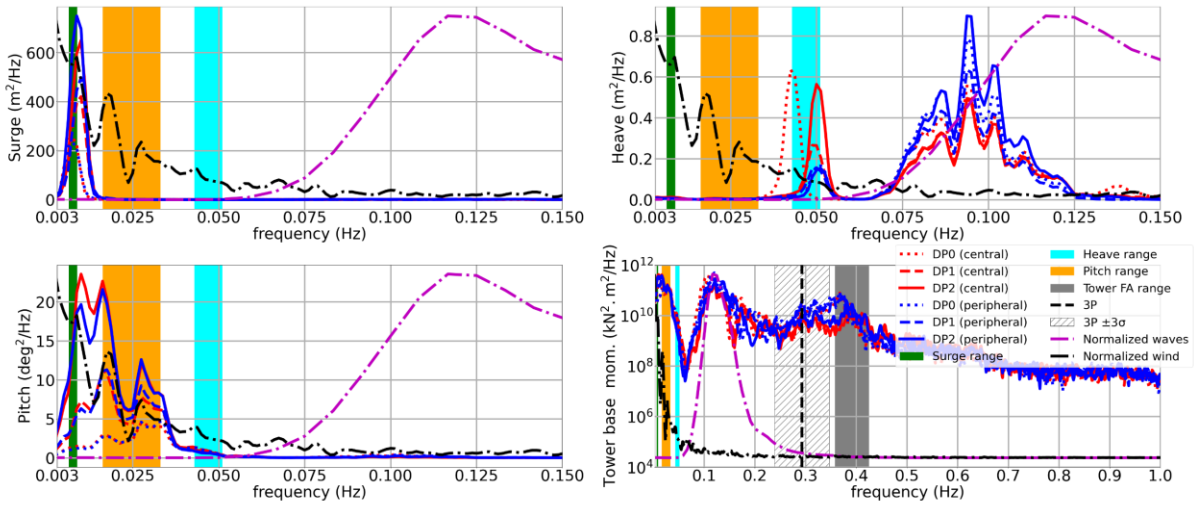

Figure 10 Above-rated condition response spectra (U = 25 m/s, H_s = 3.5 m, T_p =9 s)

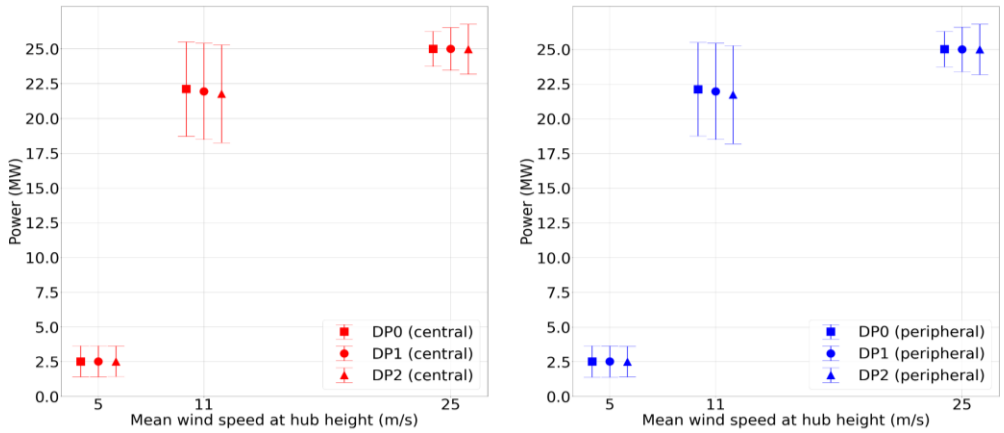

Figure 11 Mean values and standard deviations of power output

5. Conclusions

This paper presented a preliminary sizing procedure for two semisubmersible substructures to support future generation 25 MW wind turbines. The substructure designs were obtained by upscaling two existing reference platforms with central and peripheral tower configurations. The upscaling was achieved through a design space search to explore the effects of the geometrical parameters of the platforms on their basic properties including steel mass, static pitch under maximum thrust and natural frequencies of rigid body motions as well as the tower bending modes. This was achieved by developing a simplified 2D model based on eigenvalue analysis that allowed exploring a large number of design variations. The results of the parametric study show that simple theoretical upscaling based on the power ratio results in overly conservative designs with large substructure steel mass and low static pitch angle under maximum thrust. Furthermore, these designs violate the stiff-stiff tower requirement assumed in this work. By relaxing the static pitch, significant reduction in steel mass and stiffer tower was achieved.

Coupled simulations were performed for selected design points from the parametric study. Natural periods were obtained from decay tests and good agreement was found with their estimated values from the simplified model. A brief assessment of the performance of the upscaled designs was given by testing them in constant wind and three operational environmental conditions with turbulent wind and irregular waves. Results of the coupled simulations show that employing a different controller strategy to mitigate the negative damping effects around rated speed and the impact of controller detuning at above rated speeds might have the potential to significantly improve the performance of the proposed designs.

Acknowledgment

The research leading to these results has received funding from the Research Council of Norway through the ENERGIX program (grant 308839) and industry partners Equinor, AIBEL, Dr. Techn. Olav Olsen, GCE Node Service, and Energy Valley.

References

[1] IRENA 2016 Innovation outlook for offshore wind technology. International Renewable Energy Agency, Abu Dhabi

[2] Leimeister M, Bachynski E E, Muskulus M and Thomas P 2016 Rational upscaling of a semi-submersible floating platform supporting a wind turbine. *Energy Procedia*. **94**: p. 434-442.

[3] Kikuchi Y and Ishihara T 2019 Upscaling and levelized cost of energy for offshore wind turbines supported by semi-submersible floating platforms. *Journal of physics: conference series*. IOP Publishing.

[4] Zhao Z, Li X, Wang W and Shi W 2019 Analysis of dynamic characteristics of an ultra-large semi-submersible floating wind turbine. *Journal of Marine Science and Engineering*. **7**(6): p. 169.

[5] Leimeister M, Kolios A, Collu M and Thomas P 2019 Larger MW-class floater designs without upscaling?: A direct optimization approach. *International Conference on Offshore Mechanics and Arctic Engineering*. American Society of Mechanical Engineers.

[6] Ferri G, Marino E and Borri C 2020 Optimal dimensions of a semisubmersible floating platform for a 10 MW wind turbine. *Energies*. **13**(12): p. 3092.

[7] DNV 2011 Recommended practice DNV-RP-H103, modelling and analysis of marine operations.

[8] Hooft J P 1972 Hydrodynamic aspects of semi-submersible platforms.

[9] Allen C, Viscelli A, Dagher H, Goupee A, Gaertner E, Abbas N, Hall M and Barter G 2020 Definition of the UMaine VolturnUS-S Reference Platform Developed for the IEA Wind 15-Megawatt Offshore Reference Wind Turbine. National Renewable Energy Lab.(NREL), Golden, CO (United States)

[10] Gaertner E, Rinker J, Sethuraman L, Zahle F, Anderson B, Barter G E, Abbas N J, Meng F, Bortolotti P and Skrzypinski W 2020 IEA wind TCP task 37: definition of the IEA 15-megawatt offshore reference wind turbine. National Renewable Energy Lab.(NREL), Golden, CO (United States)

[11] Silva de Souza C E, Engebretsen E, Bachynski E E, Eliassen L, Berthelsen P and Haslum H 2021 Definition of the INO WINDMOOR 12 MW base case floating wind turbine. SINTEF.

[12] Wayman E N, Sclavounos P, Butterfield S, Jonkman J and Musial W 2006 Coupled dynamic modeling of floating wind turbine systems. *Offshore technology conference*. OnePetro.

[13] Abbas N, Zalkind D, Pao L and Wright A 2021 A reference open-source controller for fixed and floating offshore wind turbines. *Wind Energy Science Discussions*: p. 1-33.

[14] Gonzalez P, Sanchez G, Llana A and Gonzalez G 2015 Deliverable 1.1 Oceanographic and meteorological conditions for the design. LIFES50+